J. Physiol. (1983), **341**, *pp.* 1–24
With 9 text-figures
Printed in Great Britain

TIME DOMAIN SPECTROSCOPY OF THE MEMBRANE CAPACITANCE IN FROG SKELETAL MUSCLE

BY C. L.-H. HUANG

From the Physiological Laboratory, University of Cambridge, Downing Street, Cambridge CB2 3EG

(*Received 9 September 1982*)

SUMMARY

1. Dielectric spectra representing the frequency dependence of the complex permittivity at a range of depolarizations were obtained from voltage-clamped frog skeletal muscle membranes. This employed an analysis that derived the Fourier coefficients defining the capacitative transients to 10 mV steps as *continuous* functions of frequency, and so could examine closely the relevant frequencies at which non-linear components occurred.

2. Non-linear capacitative components were identified through their appearance at lower frequencies than those of the linear components as obtained at the −85 mV control voltage, from spectra representing a logarithmic scale of frequencies.

3. Permittivities from small depolarizing steps between about −75 and −50 mV gave single q_β dielectric loss peaks; the real permittivities declined monotonically with increasing frequency. Simple arc loci were obtained in the complex plane. With further depolarization, an additional q_γ loss peak at low frequencies and a resonant frequency in the real spectra occurred over a narrow voltage range around −45 mV. The complex loci then showed features implying an increased movement of charge not explicable through the simple effect of an electric field on a dielectric species.

4. Spectra from small hyperpolarizing steps possessed only single dielectric loss peaks and real permittivities that declined monotonically with increasing frequency. However, in the complex plane, the loss tangents at the higher frequencies implied a population of two or more dielectric relaxations.

5. The potential dependence of the frequency at maximum dielectric loss obtained from depolarizing steps showed a discontinuity at the onset of q_γ. In contrast, in hyperpolarizing responses, this dependence was smooth.

6. The q_β relaxations obtained after q_γ was abolished by 1 mM-tetracaine gave dielectric spectra that were similar whether to depolarizing or hyperpolarizing potential steps. They gave single dielectric loss peaks and semicircular complex plane loci.

7. The singularities in the dielectric spectra thus result from the q_γ charge movement component. They may reflect co-operative mechanisms that might also produce its steep voltage dependence and kinetics, and consequently those of the physiological processes it may control. These are discussed in terms of the mechanisms expected in allosteric proteins.

INTRODUCTION

A polymer molecule can be described in terms of the frequency dependence of the complex permittivity of a dielectric at any given potential (Debye, 1929; Hedvig, 1970). In such a representation, or dielectric spectrum, the *real permittivity*, ϵ', assumes a maximum value at zero frequency: this gives the maximum available capacitative charge. The value then declines with increasing frequency asymptotically towards the free-space permittivity. The *imaginary permittivity* or *dielectric loss component* ϵ'' consists of one or more peaks; these peaks characterize the different relaxations that result from the dielectric components present. It has been pointed out that large integral membrane polymers may underlie charge movements in skeletal muscle (Adrian, 1978). Furthermore, the charge movement in skeletal muscle may be made up of several components: earlier work has suggested a separation into q_α, q_β and q_γ components by virtue of their removal by tetracaine (of q_γ) or lidocaine (q_β and q_γ) (Huang, 1982; Hui, 1982) or by prolonged depolarization (Adrian & Peres, 1979). Of these components, the voltage dependence of q_γ shows a close parallel with that of contractile activation (Huang, 1982).

For these reasons a description of the non-linear charge in terms of the frequency dependence of the permittivity of a dielectric should be useful, both in a kinetic separation of these components and a description of their properties, and an earlier study has already employed such an approach (Huang, 1981*a*). The components isolated had low frequencies ($< 1{\cdot}0$ kHz) and so the spectra were deduced through an analysis of transients to small voltage steps imposed at different potentials, or *time domain spectroscopy*. This approach assumes the Fourier transform relationship between the complex permittivity in the frequency domain and the transient current obtained in response to small voltage perturbations in the time domain (Weber, 1956; Hill, Vaughan, Price & Davies, 1969).

However, in this preliminary analysis resolution of the dielectric loss peaks was limited, as was representation of the real Fourier coefficients. It was therefore not possible to examine the dielectric behaviour of charge movements in the complex plane at the frequencies where these non-linear signals occurred. This is because the fast Fourier transform performed on the 2^N sampled points of the transient is a *numerical* procedure that returns a limited number of 2^{N-1} real and 2^{N-1} imaginary Fourier coefficients for a fixed set of frequencies running from zero and incremented equally along a linear scale, up to the Nyquist frequency. Hence, while a high sampling frequency optimizes the signal-to-noise ratio in the representation of the transient, so minimizing the need for signal averaging, the discrete transform obtained in the frequency domain would represent a wide frequency band, and the low frequencies of interest would consequently be represented by few points. On the other hand, slower sampling would result in a transform with a lower Nyquist frequency, and the numerical transform would display the low frequencies more fully. However, aliasing error could then result from the higher frequency components that also may be present in the transient. The earlier study (Huang, 1981*a*) explored for sampling frequencies above which such aliasing would be minimal, but close examination of the relevant frequencies was still limited and the lower sampling rate meant a deterioration in over-all signal-to-noise ratio that had to be retrieved through

increased averaging. These restrictions confined the earlier work to demonstrating the distinct existence of q_γ and its removal by tetracaine.

This study aimed to achieve a more complete dielectric analysis by using the existence of the Fourier transform of a discrete time series representing a transient or time-limited signal as a *continuous* function in the frequency domain through a range of frequencies from zero to the Nyquist frequency. To this end, an analytical derivation of the Fourier coefficients from a time series for any chosen set of frequencies was obtained by extending the orthogonality condition for the trigonometric functions involved for periodic functions to the transient functions studied here. The complex transforms could then be displayed along a logarithmic, rather than a linear abscissa. Such a choice of axes enhanced the representation of those frequencies where q_β and q_γ occurred, while retaining an adequate representation of the higher frequencies. This close representation was possible even using a high sampling rate, which optimized the signal-to-noise ratios and so reduced the requirements for signal averaging as well.

Using this analytical approach, a full display was possible of the permittivities at frequencies relevant to the non-linear dielectric components while still preserving an adequate representation of the remaining higher frequencies. This enabled a clear resolution of the dielectric peaks corresponding to the different components of the charge movement. It was then possible to locate quantitatively the frequencies of these loss peaks, and to characterize the dielectric loss through the dependence of these peak frequencies upon the membrane potential. Finally, the close representation made possible the display of the dependence of dielectric loss upon real permittivity in the complex plane. Whereas the loci obtained from the q_β component were compatible with a simple dielectric relaxation, more complicated features occurred for the steeply voltage-sensitive q_γ component.

METHODS

Experimental procedure

Frog (*Rana temporaria*) sartorius muscle fibres were studied under a three-electrode voltage clamp at 3–6 °C. Standard (4–6 MΩ) glass micro-electrodes were inserted 500 μm (clamp electrode, voltage V_1), 1000 μm (second voltage electrode, potential V_2) and 1250 μm (current injection electrode driving current I_0) from the end of the fibre respectively. The holding potential V_H was -90 mV. The charging current to ± 10 mV steps blunted with time constant 0·2 msec superimposed 500 msec after the membrane was stepped to test voltage V'_T was measured employing the pulse procedure of Adrian & Peres (1979). If then V_T is the effective voltage about which the ± 10 mV step was being made, $V_T = V'_T \pm 5$ mV. A single experimental programme, described in Huang (1982), sampled arrays representing $V_1(t)$, $V_2(t) - V_1(t)$ and $I_0(t)$ as obtained by analogue-to-digital conversion by a C.E.D. interface (Cambridge Electronic Design, Cambridge). The arrays were transferred to central processing by an on-line PDP11/10E computer (Digital Equipment Corporation, Maynard MA U.S.A.), through which the currents were displayed as admittances of unit surface membrane area:

$$Y_m(t) = \frac{d}{6l^2 R_i} \frac{V_2(t) - V_1(t)}{\Delta V_1}.$$

Membrane capacitance was measured as the integral of the transient part of $Y_m(t)$ at the beginning and end of each voltage step. The cable constants, λ, r_i and r_m were calculated from the steady value of the voltages V_1 and V_2 and injected currents I_0 at the end of the 10 mV applied step. Calculating fibre diameter, d, and specific membrane constants R_m and C_m employed a value for R_i of 391 Ω cm in hypertonic solution at 2 °C and a Q_{10} of 1·37 (Hodgkin & Nakajima, 1972).

The sampling interval employed was 200 μsec/point giving a Nyquist frequency of 2·5 kHz. The sampling window extended over 1080 points, in which the 'on' and 'off' parts of the step both lasted 105 msec. Five to ten sweeps were averaged at each voltage at a separation of 1 sec between sweeps. Thus signal averaging was less heavy than employed earlier. Every two to three averages examining test voltages was followed by control sweeps at −90 mV; these provided control averages, and cable analysis of successive control averages checked the condition and stability of the fibre. Experiments were done in the following hypertonic solution at neutral pH: Rb_2SO_4, 5 mM; tetraethylammonium sulphate $(TEA)_2SO_4$, 80 mM; (TEA)Cl, 15 mM; $CaSO_4$, 8 mM; tetrodotoxin (TTX), 2×10^{-7} M; Tris buffer, 3 mM; sucrose, 350 mM. The pharmacological studies employed 1 mM-tetracaine. Fibres were examined within 1–1½ hr of substitution of the above bathing solution for the isotonic Ringer solution in which the fibres were dissected.

In the earlier study (Huang, 1981*a*) sweeps for cable constant evaluation and time domain representation, and averages for Fourier analysis were obtained in separate procedures. In this study, the same arrays were obtained at a close sampling interval for both analyses as it was not now necessary to vary the sampling frequency to adjust the frequencies being examined.

Analysis

The analysis procedure employed assumes that the complex permittivity of a dielectric as a function of frequency, or its dielectric spectrum, is the Fourier transform of its transient current response to an applied voltage step (Hedvig, 1970; Hill *et al.* 1969; Weber, 1956). The procedure to be described was performed on the transients to *either* the depolarizing *or* the hyperpolarizing parts of the imposed voltage steps, and over an interval (100 msec) sufficiently long to allow the transient to relax fully.

Before the actual transform procedure, leaks and delayed rectifier currents were corrected for (Huang, 1981*a*). The zero phase-shift condition (Bracewell, 1978) was achieved by 'rotating' the experimental arrays, making the first point for transformation coincide with the beginning of the transients, which were expressed as admittances of unit surface membrane area in floating point form. The complex permittivities obtained were accordingly represented as capacitances of unit surface membrane. The scaling theorem correction was implicit to the transform procedure, as described below. The complex permittivities were then derived by evaluating the array $\{a_n, b_n\}$ of cosine and sine coefficients for a chosen set of frequencies $\{f_n\}$ in the trigonometrical series describing analytically the *transient* part of the response being examined (Lighthill, 1958):

$$h(q\Delta t) = \sum_{n=0}^{n=\infty} (a_n \cos(q\pi F_n) + b_n \sin(q\pi F_n)). \quad (1)$$

The above half-range trigonometric expansion represents the qth value of the real function $h(t)$ as sampled at intervals Δt, Nyquist frequency $f_c = 1/(2\Delta t)$. F_n is the nth frequency point, f_n, as normalized to the Nyquist frequency, $F_n = f_n/f_c$.

For a time-limited function, coefficients $\{a_n, b_n\}$ can be obtained as continuous solutions at any frequency although, for a discrete time series, the solving functions will be periodic in the frequency domain over twice each Nyquist frequency, f_c. This situation is different from the fast Fourier transform analysis of functions periodic in time, where achieving a finite sampling window necessitates truncating the function through an interval that gives a fundamental period, T_0. This corresponds to convolution of the analytical transform with the filtering function $\sin(2\pi fT_0)/2\pi fT_0$, so producing a ripple error that is absent only at a discrete set of frequencies f_n that are integer multiples of the fundamental, $f_0 = 1/T_0$. Additionally some form of window would also be necessary to minimize harmonic distortions due to leakage error from frequency components of the periodic functions for which the sampling period is not a multiple of their fundamental period. In contrast, for time-limited functions, provided the sampling period exceeds the duration over which the absolute value of the function is greater than zero, integration of the sine and cosine terms describing $h(t)$ over this interval is equivalent to an integration over infinite time. There is therefore no ripple or leakage error.

Therefore, harmonic analysis then can solve for the Fourier coefficients $\{a_n, b_n\}$ for *any* set of normalized frequencies $\{F_n\}$, by assuming the orthogonal properties in the trigonometric functions involved. These give:

$$a_n = \frac{2}{T_0}\int_0^{T_0} h(t)\cos(\pi F_n t/\Delta t)\,dt$$

$$= \frac{2\Delta t}{T_0}\sum_q h(q\Delta t)\cos(q\pi F_n) \tag{2}$$

$$b_n = \frac{2}{T_0}\int_0^{T_0} h(t)\sin(\pi F_n t/\Delta t)\,dt$$

$$= \frac{2\Delta t}{T_0}\sum_q h(q\Delta t)\sin(q\pi F_n). \tag{3}$$

Note that the above representations for the values of a_n and b_n assume that the sampling points are equally spaced. The coefficients $\{a_n, b_n\}$ were now related analytically to corresponding values on the *continuous* Fourier transform $H(f)$: applying the appropriate trigonometrical identities to eqn. (1) gives:

$$h(q\Delta t) = \frac{a_0}{2} + \frac{1}{2}\left[\sum_{n=1}^{\infty}(a_n - jb_n)\exp(jq\pi F_n) + \sum_{n=1}^{\infty}(a_n + jb_n)\exp(-jq\pi F_n)\right]. \tag{4}$$

If $F_n = -F_{-n}$, then a_n is even, and b_n is odd:

$$a_n = a_{-n}, \quad b_n = -b_{-n}. \tag{5}$$

This gives

$$\sum_{n=1}^{\infty} a_n \exp(-j\pi q F_n) = \sum_{n=-1}^{-\infty} a_n \exp(j\pi q F_n), \tag{6}$$

and

$$\sum_{n=1}^{\infty} jb_n \exp(-j\pi q F_n) = -\sum_{n=-1}^{-\infty} jb_n \exp(j\pi q F_n). \tag{7}$$

From eqns. (4), (6) and (7),

$$h(q\Delta t) = \sum_{n=-\infty}^{\infty} \alpha_n \exp(j\pi q F_n), \quad \text{where} \quad \alpha_n = \frac{a_n - jb_n}{2}, \quad \text{and} \quad n = \pm 1, \pm 2\ldots \tag{8}$$

From eqns. (2), (3), (6) and (7), α_n is the *continuous* function

$$\alpha_n = \frac{1}{T_0}\int_0^{T_0} h(t)\exp(-j\pi F_n t/\Delta t)\,dt, \quad n = 0, \pm 1, \pm 2\ldots \tag{9}$$

and provided $h(t)$ is zero outside the limits $(0, T_0)$, then the array of cosine and sine coefficients, $\alpha_n \equiv \{a_n, b_n\}$ gives the value of the transform at a particular frequency f_n:

$$H(f_n) = \int_{-\infty}^{\infty} h(t)\exp(-j2\pi f_n t)\,dt = \frac{T_0}{2}(a_n - jb_n). \tag{10}$$

The transform, $H(f_n)$ was thus obtainable from the original discrete time series $h(q\Delta t)$ through assuming the following.

(i) The cosine and sine trigonometric functions form orthogonal systems under the conditions employed. The orthogonality is well known to be the case in periodic functions. In the present work, the transient parts of the 'on' and 'off' responses were transformed as separate time series, and so transforms derived from depolarizing and from hyperpolarizing parts of the steps were obtained separately. The time series being considered here were therefore of time-limited functions that could be represented within a finite interval. Such functions can be considered as being periodic, but in which the period is infinity. Their Fourier coefficients accordingly remain available (and, under such circumstances, as continuous functions of frequency) through the same orthogonality conditions, essentially as demonstrated for periodic functions.

(ii) The particular range of frequencies under which the coefficients can be obtained using such an approach is determined by the sampling rate of the analogue-to-digital conversion process.

Sampling the originating function $h(t)$ at intervals Δt, gives a time series $\hat{h}(t)$ which is the product of $h(t)$ with a series of equally spaced singular functions $\Sigma_{s=-\infty}^{+\infty} \delta(t-s\Delta t)$. The corresponding function in the frequency domain $\hat{H}(f)$ is the convolution of the desired transform, $H(f)$, with the periodic singular function $(1/T)\,\Sigma_{u=-\infty}^{\infty} \delta(f-u/\Delta t)$. $\hat{H}(f)$ is therefore periodic in the frequency domain over interval $1/\Delta t$, and so the analysis described here gives the values of the Fourier coefficients over only *one* such period, in the interval $0 < |f| < 1/2\Delta t$.

(iii) The sampling intervals employed were sufficiently close to justify the equivalence of the continuous and discrete forms of the integrals in eqns. (2) and (3). This assumption is justified provided $h(t)$ did not have frequency components beyond $\pm f_c$. The originating function would then be fully specified by values sampled at equal intervals not exceeding $1/(2f_c)$, apart from any harmonic terms with zeros at the sampling points. Aliasing error that would result from insufficiently close sampling therefore remains the major remaining source of distortion when analysing time-limited signals. However, the sampling frequency in this study was kept at a fixed high value corresponding to a Nyquist frequency of 2·5 kHz. This is over five times the frequency range (0–300 Hz) over which the relatively low-frequency non-linear signals occurred (Huang, 1981*a*). Furthermore, before analogue-to-digital conversion, the signal was filtered through low-pass three-pole Butterworth filters (Barr & Stroud, London) set at a corner frequency of 1 kHz, and so aliasing error was minimized in both linear and non-linear parts of the signal as far as possible.

(iv) The functions analysed were zero everywhere outside an interval falling entirely within the limits of integration. Thus the transients were always sampled until they had relaxed fully from the applied voltage steps.

Using this analysis, a sufficient representation of the complex permittivities was achieved when they were displayed as 167 positive real and 167 positive imaginary coefficients with frequency represented along a logarithmic abscissa from 10^{-1} Hz up to the Nyquist frequency. Both spectra and complex plane loci were dimensioned in $\mu F/cm^2$ and displayed using a Bryans A3 plotter driven by the digital-to-analogue converter of the computer interface.

RESULTS

Unsubtracted dielectric spectra

Most of the results concern the non-linear permittivities as obtained from subtracting control dielectric spectra deduced from ± 10 mV steps about a membrane potential of -85 mV, from those at the test voltages V_T. However, certain features of importance were obtained only from unsubtracted spectra obtained by analysing entire transients. Fig. 1 shows results from 10 mV depolarizing steps, imposed through a range of voltages, V_T, including the reference potential of -85 mV; the plots show: *A*, the real permittivities ϵ'; *B*, the imaginary permittivities or dielectric loss ϵ'' as functions of the frequency of a driving field, on a logarithmic scale of frequency; *C*, the dependence of ϵ'' upon ϵ' as loci in the complex plane. The results are dimensioned as capacitances of unit surface membrane area and are represented for frequencies between 0·1 Hz and 2·5 kHz. They demonstrate that the sampling and filtering procedures chosen in the experiments were unlikely to have produced appreciable aliasing error or other sources of harmonic distortion in the results. The sampled signals were real and causal time-limited discrete functions and so the real part of their Fourier transforms would be even, and the imaginary parts odd functions of frequency. Additionally, the complex transforms can be assumed to represent the electrical properties of a dielectric material and so, under the sign convention used here, both ϵ' and ϵ'' would be positive, but would approach zero at high frequencies. Therefore aliasing would have augmented the real, and diminished the imaginary parts of the spectra through reflexion of these respective functions on their ordinates

at the Nyquist frequency (Papoulis, 1977). The presence of aliasing consequently would have been inferred had the real permittivities not approached zero towards the Nyquist frequency (cf. Huang, 1981*a*). This did not occur experimentally.

The dispersions resulting from the presence of potential-dependent capacitance produced loss peaks at relatively low frequencies, below about $f = 100$ Hz (Fig. 1*B*). The frequency range selected spanned the dispersion range of the dielectric properties

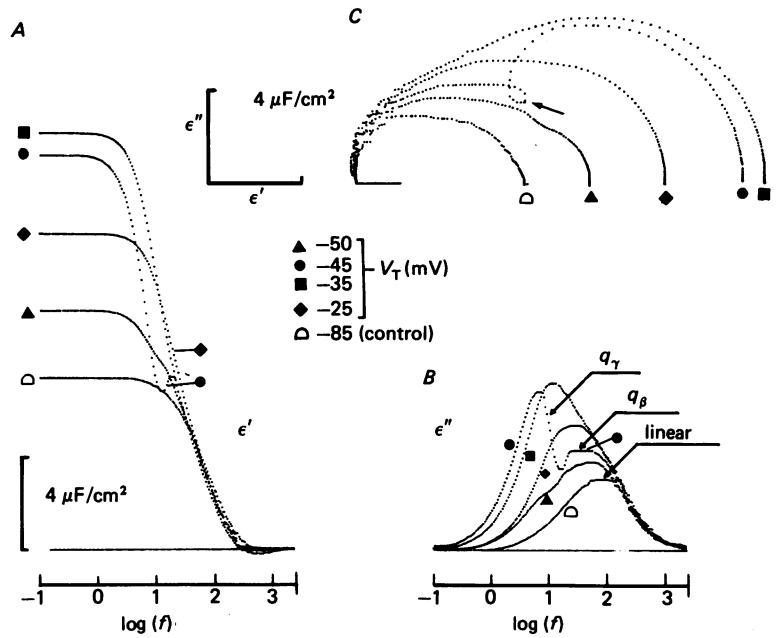

Fig. 1. Muscle dielectric properties as deduced from analysis of unsubtracted transients obtained from applied 10 mV depolarizing steps about a series of depolarizing voltages, V_T. *A*, real permittivities, ϵ'. *B*, imaginary permittivities, or dielectric loss, ϵ''. The horizontal lines represent 0 μF/cm². The spectra are represented along a logarithmic frequency scale running from 0·1 Hz to the Nyquist frequency of 2·5 kHz. *C*, locus of ϵ'' as a function of ϵ' in the complex plane. The short horizontal line marks the ϵ' abscissa. Fibre cable constants: R_i, 338 Ω cm; λ, 3·15 mm; r_i, 4694 kΩ/cm; diameter, 95 μm; r_m, 465 kΩ cm; R_m, 14·0 kΩ cm²; C_m, 7·5 μF/cm².

of the muscle membranes being examined, and resulted in a detailed representation of those frequencies at which the dielectric loss was most prominent, while simultaneously preserving satisfactory representation of the entire frequency band available. The non-linear dielectric properties therefore were represented in the frequency domain very prominently as one or more peaks distinct from the linear components, the latter being the major part in the spectra obtained about the reference potential of −85 mV. Thus, even in unsubtracted spectra, the different components could be distinguished clearly (Fig. 1*B*, arrows).

First, there was the permittivity at the −85 mV reference potential. As this reflects mainly linear properties resulting from membrane geometry and capacitance, it was used to compare with spectra obtained at other voltages in their interpretation. This had a loss maximum at around 100 Hz. In terms of the equivalent linear process,

this corresponds to a relaxation of time constant around 1·5 msec, and so would be consistent with the series R–C circuit used to describe impedances due to the membrane of the transverse tubular system (Falk & Fatt, 1964). Components of higher frequency than this would not be expected to be represented distinctly owing to the use of blunted potential steps and the low-pass filtering required in the experiment procedure (see Methods).

Secondly, the voltage-dependent components occurred as additive contributions to the spectrum at −85 mV. A loss peak, due to the q_β component (see Fig. 1 *B*) occurred in the frequency range 30–60 Hz and was especially distinct in the spectra at −50 and −45 mV. There was also a lower-frequency loss peak due to q_γ at very low frequencies around 5–15 Hz at around −45 mV in the Figure, and also at potentials depolarized to this. Examination of the dielectric loss, ϵ'', as a function of frequency therefore clearly distinguished the voltage-dependent capacitative components from the linear admittances by virtue of the lower frequencies at which their loss peaks occurred. This was possible even in unsubtracted transforms.

The values of the real permittivities assumed their maximum values at low frequencies below about 1·0 Hz (Fig. 1 *A*). The real value of the Fourier transforms at the zero frequency ordinate gives the integral of the originating transient (Bracewell, 1978), and so also gives the size of the effective membrane capacitance (Adrian & Almers, 1974). The non-linear capacitative components thus made a large contribution to the measured membrane capacitance. For example, at a potential of −35 mV, the existence of the charge movement more than doubled the capacitance when this was compared to that at the −85 mV reference voltage. As the frequency is increased, the magnitude of real permittivity of a dielectric material would be expected to decline, and this was generally the case. However, in the experimental results, the spectrum of the real permittivities, ϵ', showed a local peak at potentials around −45 mV, and this was consistent with a component (absent in the −85 mV controls) that contained a resonant frequency. This change coincided with a sharp increase in the low-frequency capacitance; these phenomena are considered in more detail below.

Using the logarithmic frequency scale made it possible to achieve a satisfactory representation of the dependence of the dielectric loss, ϵ'', upon the real permittivity ϵ' as a series of loci in the complex plane (Fig. 1 *C*). In analyses of this kind, first-order relaxations would produce semicircular loci in the ϵ' dispersion region, which would transect the abscissa at right angles, provided the membrane is uniformly polarized (Cole, 1968). However, the experimental locus at the −85 mV reference potential was a depressed arc, and this implies a population of relaxations involving more than one time constant. This may reflect linear contributions from surface as well as transverse tubular membrane. Additionally there exists the q_α charge (see Adrian & Peres, 1979; Huang, 1981*b*) which is at its largest in this range of voltages. Nevertheless, through the voltages examined, all the loci in the complex plane transected the abscissa at close to right angles. This is as would be expected for a uniformly polarized dielectric; the existence of cable effects resulting from any non-uniform voltage clamping would have produced an infinite number of relaxations, which would have made the loss angle considerably less than 90° at the high frequencies (Falk & Fatt, 1964). Satisfactory uniformity of membrane polarization in the three-electrode voltage-

clamp method has also been indicated by earlier comparisons between input admittances predicted for an equivalent circuit used to describe a uniformly polarized membrane, and the same circuit in the geometry entailed by the voltage clamp. The predicted admittances closely matched between frequencies of 0 and 2·5 kHz with minimal distortion (Huang, 1981*b*).

At potentials depolarized to −85 mV, the complex plane loci increased in radius. This reflects the existence of potential-sensitive capacitances: the distance between the two intercepts on the real abscissa gives the total capacitative charge. The increase in effective capacitance was especially marked at −45 mV, and this increase coincided with a 'loop' in the locus (Fig. 1*C*, arrow); these singular features are discussed in detail below.

The analysis procedure used represents a substantial improvement over what would have been obtained from a standard fast Fourier transform algorithm. Fig. 2 shows an analysis of that transient at −45 mV whose transform is also shown in Fig. 1. The standard algorithm *cannot* provide Fourier coefficients for any chosen set of frequencies, but rather represents a set of frequencies incremented uniformly from zero to the Nyquist frequency. In consequence, whereas the analysis in Fig. 1, by employing an appropriate logarithmic scale, displayed the low frequencies of interest in detail and compressed the high frequencies, in Fig. 2 the frequencies were represented on a linear scale from zero to the Nyquist frequency. The consequence of this was that the low frequencies are now represented by only very few points. As a result, neither the relevant q_β and q_γ loss peaks (Fig. 2*A*), nor the resonance features in the real permittivities were demonstrable at −45 mV. The difference spectra (Fig. 2*C*) are to be compared with those obtained at −45 mV in Fig. 3. They certainly do not show the distinct dielectric peaks in Fig. 3. Finally, although the loci in the complex plane in Fig. 2*D* and *E* show the high-frequency points, they entirely omit the low frequencies at which the non-linear effects occur.

Non-linear permittivities: depolarizing steps

The spectra from whole transients enabled identification of linear and non-linear parts of the dielectric response, and confirmed that errors due to cable attenuations or other signal problems were minimal. However, ideally the non-linear signals should be examined in the absence of contributions from the linear components. This condition was approximated by subtracting the reference spectrum as obtained from a perturbation at −85 mV from the spectra obtained at the test voltages. In both cases, the perturbing step was 10 mV, as in earlier work. The addition theorem for functions in the frequency domain implies that the resulting difference spectrum does isolate the non-linear components (Bracewell, 1978). However, even the reference spectrum itself would have contained appreciable non-linear charge, which may account for as much as 25 % of the total capacitance (Huang, 1981*b*; Duane & Huang, 1982). Nevertheless, this extra charge was mainly due to the q_α component, whose voltage dependence is considerably less than that of q_β and q_γ, particularly over the potential range examined here (Huang, 1982) and so the consequent errors would be small.

Fig. 3 shows *A*, real ϵ' and *B*, imaginary permittivities, ϵ'' as functions of frequency, deduced from transient responses to 10 mV depolarizing steps about different test

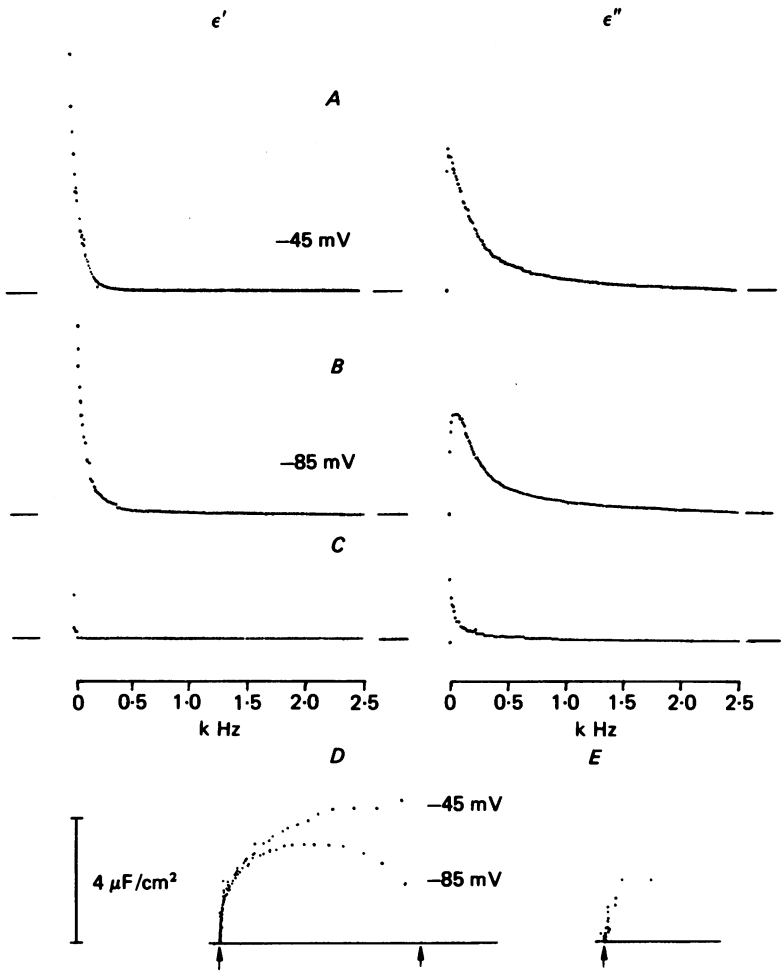

Fig. 2. Dielectric analysis of capacitative transients at a test voltage of −45 mV and a control voltage of −85 mV. Same sampled transients as in Fig. 1, but analysis used a standard fast Fourier transform algorithm. Real (left, ϵ') and imaginary (right, ϵ'') permittivities at *A*, the −45 mV test potential and *B*, the −85 mV control. *C*, difference between permittivities obtained at −45 and −85 mV. The standard algorithm gave 256 Fourier coefficients along a linear scale from 0 to the 2·5 kHz Nyquist frequency. The non-linear components of interest were poorly represented and little of the detail offered by Fig. 1 is available. The horizontal lines represent 0 μF/cm². *D*, complex plane representation of the transients entirely misses the low frequency points of interest. *E*, the non-linear complex plane plot is incomplete. The arrows mark the origins, and the value of the control capacitance. The traces have been retouched for clarity.

voltages V_T from which reference spectra were subtracted. The use of a logarithmic abscissa from 10^{-1} Hz up to the Nyquist frequency of 2·5 kHz gave a preferential representation of the lower frequencies and so displayed clearly the non-linear dielectric loss peaks, but at the same time preserved adequate presentation of the entire frequency range. Between the voltages of −65 and −50 mV, there was only the q_β peak in the dielectric loss (Fig. 3*B*), and at these potentials the real permittivity (Fig. 3*A*) declined monotonically with increasing frequency towards zero, as would be expected for relaxations of dipole orientations in a dielectric.

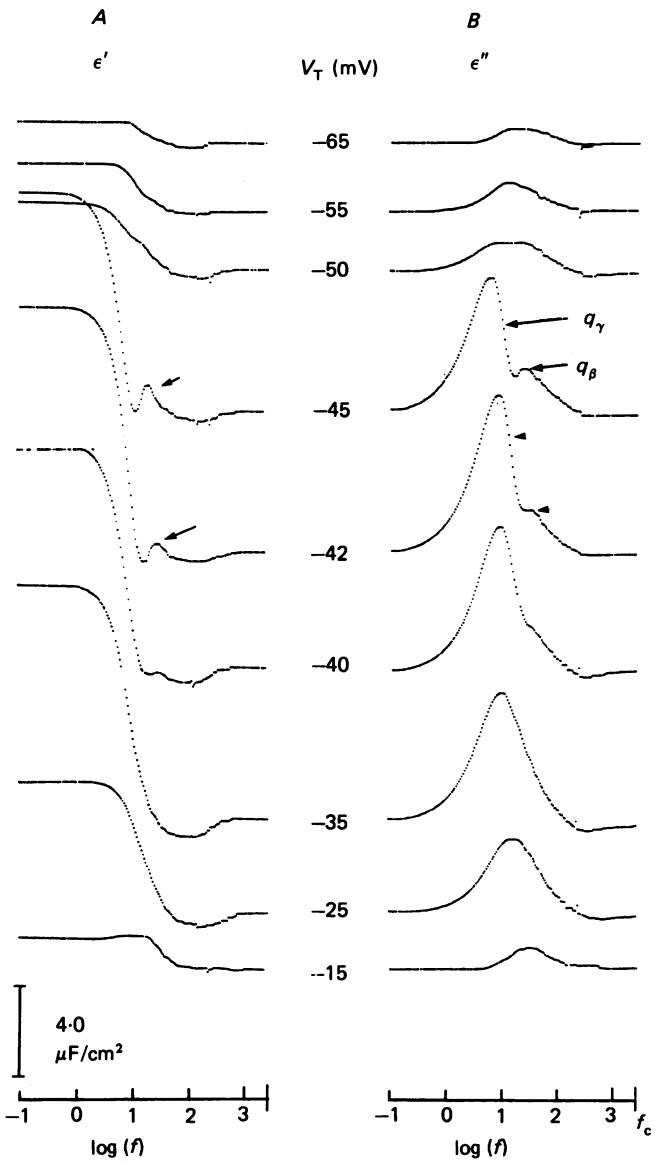

Fig. 3. Frequency dependence of the non-linear complex permittivity at different voltages V_T obtained from current transients to small depolarizing steps. Both *A*, real (ϵ') and *B*, imaginary (ϵ'') permittivities are displayed along a logarithmic abscissa between 10^{-1} Hz and the Nyquist frequency of 2·5 kHz. The arrows mark the q_β and q_γ imaginary peaks (*B*), and the inductive behaviour in the real spectra (*A*).

However, the spectra showed singular behaviour with the onset of the q_γ component of the charge movement. Over a narrow range of voltages around −45 mV, a large additional q_γ dielectric loss peak occurred at low frequencies around 3−5 Hz (Fig. 3*B*, arrowed). This onset of q_γ was associated with a sharp increase in the low-frequency real permittivity, and therefore in the total available amount of non-linear charge (Fig. 3*A*). Thus, whereas q_γ is often difficult to detect from inspection of records in the time domain, it is very strikingly represented in the frequency domain, even

though the two domains are merely different representations of essentially the same information. This is because for the q_γ transient expressed as a function of time, the ratio of its definite integral to its ordinate at time zero, or *equivalent width*, is large. The equivalent width of a transform is the reciprocal of that of its originating function

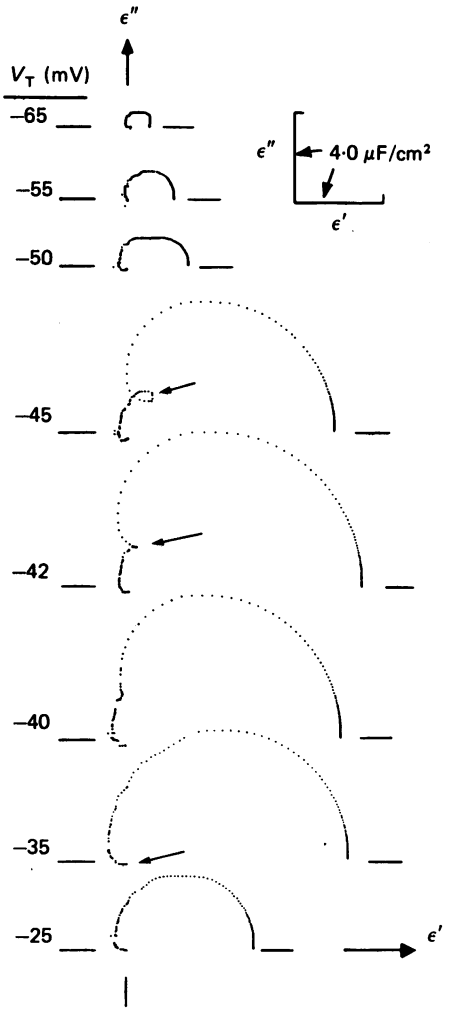

Fig. 4. The complex permittivity, as deduced from small (10 mV) depolarizing steps about a range of voltages, V_T, represented as loci in the complex plane. The results are dimensioned as capacitances of unit surface membrane area. The vertical lines mark the position of the imaginary (ϵ'') ordinate, and the horizontal lines the real (ϵ') abscissae. The singular behaviour in the loci beyond −45 mV is arrowed.

in the other domain (Bracewell, 1978). The q_γ spectrum accordingly appeared as a prominent and narrow low-frequency peak, while its large capacitative contribution produced a marked increase in the value of the real permittivity at zero frequency.

With further depolarization, the q_γ peak broadened and its peak shifted to higher frequencies, thereby merging with the wider q_β peak (Fig. 3*B*). The q_γ component thus appears abruptly in the dielectric loss in the low frequencies at sharply defined

potentials, and these are close to both the contractile rheobase as obtained using identical pulse procedures (Huang, 1981*c*), and the onset of demonstrable calcium-related optical transients (Kovacs, Rios & Schneider, 1979). Thus, examination of the imaginary permittivity reinforces the notion derived from earlier steady-state studies (Huang, 1982) of a relationship between q_γ and contractile activation.

Features of interest in the real spectrum (Fig. 3*A*) were also attributable to q_γ. For a first-order dielectric process, the real coefficients would have declined monotonically with increasing frequency and this dependence would pass through inflexions coinciding with the dielectric loss maxima. This was not the case when q_γ was present, where there appeared superimposed prominent biphasic peaks in the real permittivities. For example, in Fig. 3*A*, at −45 mV, the q_γ loss peak at $f = 3{\cdot}7$ Hz was associated with a biphasic component at 10–15 Hz in the real spectrum (Fig. 3*A*, arrowed). This phenomenon is not consistent with a simple dielectric description of the system, in that the equivalent circuit representation of such results would entail inclusion of a voltage-dependent inductance, in addition to the capacitative component (Von Hippel, 1954).

Closer insight into the nature of this anomalous dispersion due to q_γ was achieved by representing the dependencies of the non-linear dielectric loss, ϵ'', upon the corresponding real permittivity, ϵ', as loci in the complex plane. Fig. 4 shows such a series of loci over a range of test voltages. As the reference −85 mV permittivities had previously been subtracted, the plots represent the behaviour of the non-linear components only. At all the voltages, the loci transected the ϵ' abscissa at right angles at the low frequencies.

At small depolarizations not beyond −50 mV, the loci traced depressed semicircular arcs, as would be expected of the dielectric properties of one (or more) polymer species (see Discussion). The angle subtended by the line joining the origin with a defined point on the arc and the abscissa gives the argument of the locus, at the frequency concerned. This corresponds to the phase angle, δ, in the dielectric displacement vector **D** had the system been subject to a steady-state sinusoidal imposed field **E**. In situations of this latter kind, external work is dissipated only by that part of the displacement current in phase with the imposed voltage. Hence the dielectric loss tangent, tan δ, which for any given frequency is the ratio ϵ''/ϵ', gives the energy dissipated normalized to that stored in each cycle (Hill *et al.* 1969). The loci obtained at the small depolarizations therefore correspond to a monotonic increase in this value as the frequency increases, in addition to demonstrating the decline in the real permittivity. A semicircular arc plot would have corresponded to that case involving a simple Eyring system of two steady-state levels separated by an activated state, with the energy of each state a single valued function of the voltage. On the other hand, the depressed arc loci observed are consistent with the presence of a population of two or more such relaxations.

However, at stronger depolarizations the loci obtained deviated from this simple pattern. For example, at a membrane potential of −45 mV, there occurred a 'loop' in the locus obtained (Fig. 4, arrowed). This was coincident with the onset of the q_γ dielectric loss peak, and may therefore be the result of mechanisms involved in the q_γ charge movement. Such features as occurred in the loci implied a decrease in the dielectric loss tangent over the frequencies concerned and so deviate from the

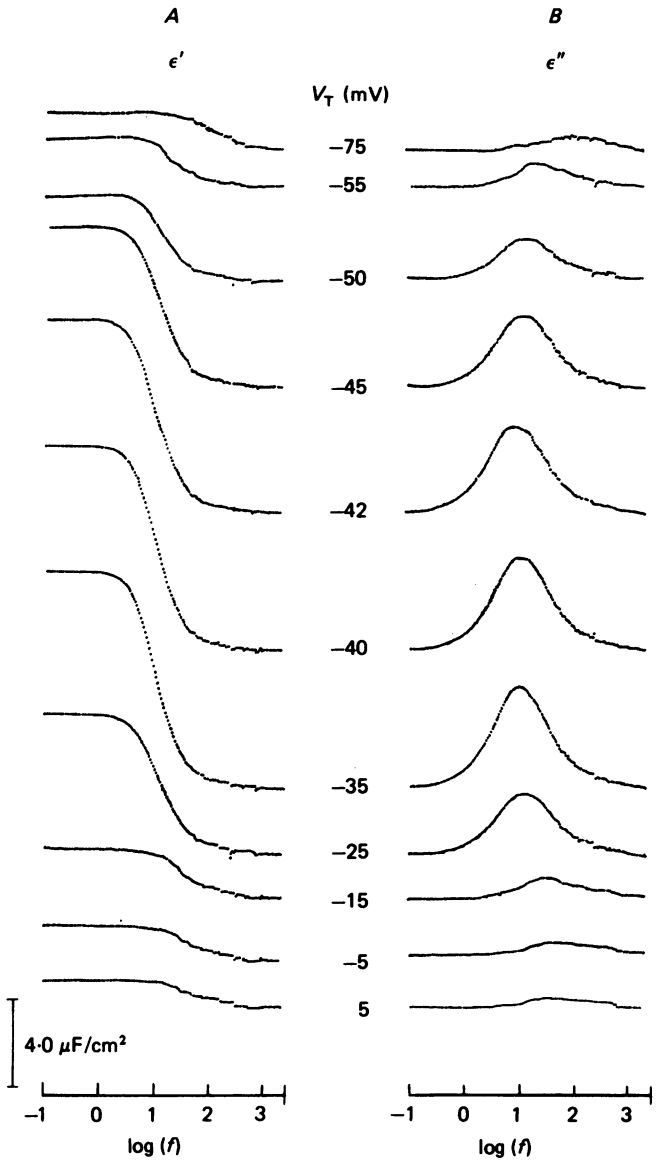

Fig. 5. Dielectric spectra representing the non-linear part of A, the real (ϵ') and B, the imaginary permittivity (ϵ'') at different voltages obtained from current transients to 10 mV hyperpolarizing steps. The logarithmic frequency scale runs from 10^{-1} Hz to the Nyquist frequency of 2·5 kHz. The Figure has been retouched for clarity.

simple monotonic increase expected from a straightforward dielectric dispersion. With stronger depolarization, as at −35 mV, the effect tended towards higher frequencies, at which the complex loci then left the permittivity quadrant. As pointed out earlier, these findings imply a larger amount of net charge movement than would be expected for a particular amount of energy dissipation in the cycle in comparison to what would be predicted for a first-order dielectric relaxation at the frequencies involved. If one still assumes that q_γ originates fundamentally from a capacitative

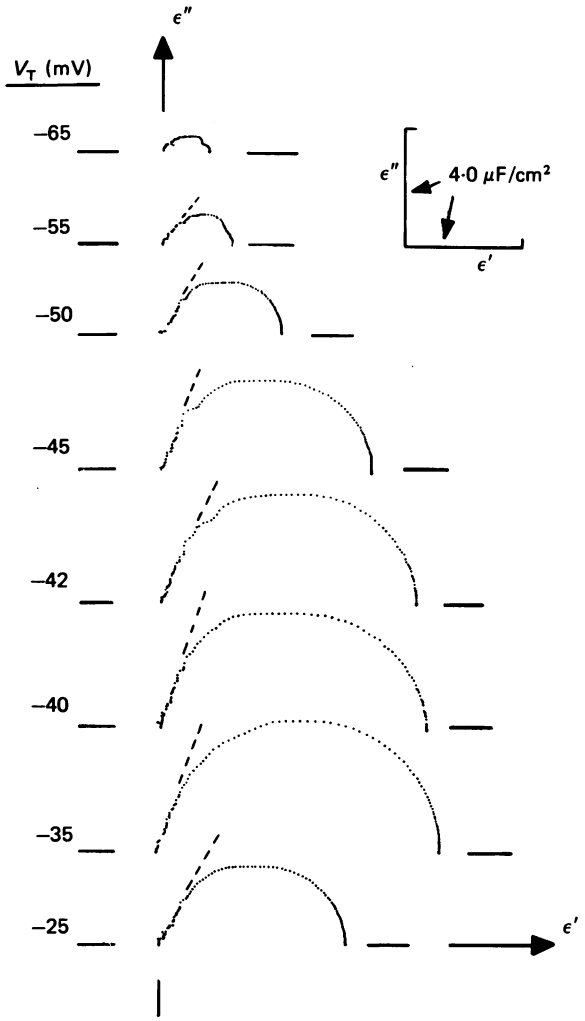

Fig. 6. Complex plane loci of the dependence of the dielectric loss, ϵ'', upon the real permittivity, ϵ', deduced from responses to 10 mV hyperpolarizing steps, dimensioned in $\mu F/cm^2$, over a range of depolarizing voltages, V_T. The vertical lines indicate the ϵ'' ordinate, and the horizontal lines the ϵ' abscissa. The dotted lines approximate the tangents giving the high frequency phase angles.

rather than an inductive or resistive mechanism (Huang, 1983), then the simplest explanation for these findings would be for the existence of co-operative effects enhancing the underlying transitions in response to applied fields at certain frequencies. Such a notion would be consistent with the coincident sharp increase in total conserved charge reported at the threshold of q_γ.

Non-linear permittivities: hyperpolarizing steps

When small hyperpolarizing steps were applied through the same voltage range, the complicated behaviour resulting from depolarizing steps, as described above, did not occur. The frequency dependence of the deduced permittivity (Fig. 5) paralleled that expected for a simple dielectric material. The real permittivities, ϵ', fell

monotonically towards zero with increasing frequency, from a value at low frequency equal to the total available capacitative charge: the resonant frequencies demonstrated above for the responses to depolarizing steps were absent (Fig. 5*A*). There was only one dielectric loss peak in the range of potentials examined (Fig. 5*B*). Its position was clearly dependent on voltage, assuming lower frequencies in the middle of the voltage range than at strongly depolarized or hyperpolarized potentials. However, it neither separated into two components nor reached frequencies as low as the q_γ peak in the depolarizing responses. The dependence of ϵ'' on ϵ' in the complex plane (Fig. 6) was a simple arc locus, and so implied a loss tangent monotonically increasing with frequency. However, the loss tangent at the higher frequencies of the arc approached between 50° and 70°, and never reached 90° (Fig. 6, dotted lines). This finding suggests the existence of a population of two (or more) relaxation times in place of the co-operative effects implied by the depolarizing spectra. Certainly, for reasons given in previous sections, it is unlikely that the low angle in this case reflects artifacts from cable effects.

The considerable differences implied in the mechanism underlying transients to depolarizing as opposed to hyperpolarizing steps were especially clear on comparing the frequencies of their dielectric loss peaks (Fig. 7). These were expressed as the reciprocal of the angular frequency at the loss maxima, ω_p^{-1}: such an approach has been employed elsewhere to characterize the dielectric loss in a wide range of materials (Dissado & Hill, 1979; Jonscher, 1975). For a system possessing two steady-state levels, as has been deduced earlier for the q_γ and q_β charge movement components (Duane & Huang, 1982), the expected dependence of ω_p on potential (Hedvig, 1970) in a simple Eyring system is:

$$\omega_p^{-1} = A/[\exp((\bar{\epsilon}_1 - \bar{\epsilon}_a)\, q/ekT) + \exp((\bar{\epsilon}_2 - \bar{\epsilon}_a)\, q/ekT)].$$

The symbols e, k, and T take their usual physical meanings; A is the Arrhenius constant, and q is the total available dipole moment, normalized to the membrane thickness at the voltage concerned. The terms $\bar{\epsilon}_1$, $\bar{\epsilon}_2$ and $\bar{\epsilon}_a$ are the respective energies of the levels $j = 1$, $j = 2$ and the activated complex $j = a$. They can be represented as virial expansions possessing constant coefficients, of the applied voltage, V, and therefore are smooth functions of the potential across the membrane. Hence the term ω_p^{-1} would also be expected to vary smoothly with potential in such a system. However, this was not the case for the dielectric loss peaks deduced from the depolarizing steps. Thus, at potentials between -80 and -55 mV, ω_p^{-1} was around 10 msec/rad or below. However, between -55 and -45 mV, the frequency of maximum dielectric loss appeared to traverse a discontinuity, which is illustrated in Fig. 7*A* for some of the individual fibres studied by the dotted lines. The latter resulted in a large increase in ω_p^{-1} to values of 20–30 msec/rad. However, further depolarization then resulted in a sharp fall in ω_p^{-1}, implying a strong voltage dependence in the q_γ process it represents.

Neither the discontinuity in this dependence, nor the decrease in ω_p^{-1} with further depolarization from the potential at which the discontinuity appeared was consistent with the expectations from a straightforward Eyring system (see Adrian, 1978). In contrast, the discontinuity did coincide with the co-operative mechanisms as implied in the complex plane plots, as well as the onset of the q_γ loss peak. These findings

differed from those obtained for frequency peaks in hyperpolarizing responses (Fig. 7*B*), where the dependence on voltage was smooth, showing maxima at around −40 mV, in agreement with the transition potential of the charge movement recorded under similar conditions (Huang, 1982). These latter findings are as expected for a system comprising one (or more) simple dielectric relaxations.

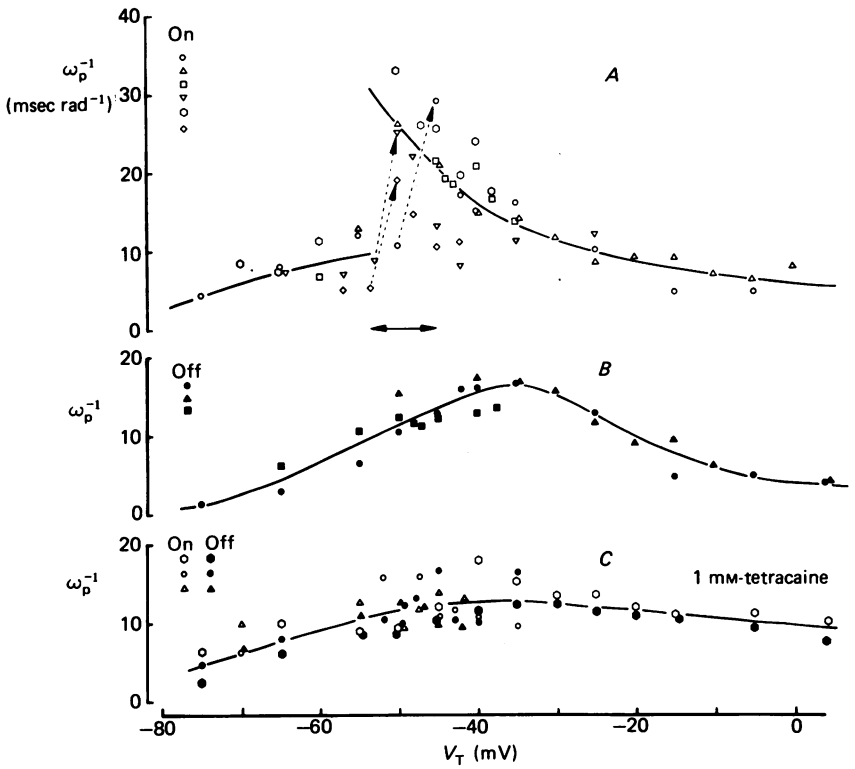

Fig. 7. Voltage dependence of the frequency of maximum dielectric loss represented as reciprocal angular frequency at the peak ω_r^{-1} (msec/radian) in: *A*, muscle fibres subject to depolarizing voltage steps; *B*, muscle fibres subject to hyperpolarizing voltage steps; *C*, muscle fibres subject to either sort of step, in 1 mM-tetracaine. Cable constants: *A*, six fibres, temp. = 3·8±0·48 °C, R_i = 367±5·0 Ω cm, λ = 2·2±0·39 mm, r_i = 6448±1121 kΩ/cm, diam. = 89·9±8·5 μm, r_m = 324±109 kΩ cm, R_m = 8·86±3·0 kΩ cm², C_m = 9·6±1·07 μF/cm²; *B*, three fibres, temp. = 3·8±0·38 °C, R_i = 337±4·0 Ω cm, λ = 2·9±0·51 mm, r_i = 4426±707·3 kΩ/cm, diam. = 103±10·8 μm, r_m = 470±183·6 kΩ cm, R_m = 13·5±4·64 kΩ cm², C_m = 10·52±1·92 μF/cm² *C*, four fibres, temp. = 4·2±0·09 °C, R_i = 333±0·87 Ω cm, λ = 2·8±0·04 mm, r_i = 7434±724·6 kΩ/cm, diam. = 82·5±4·65 μm, r_m = 528±71·4 kΩ cm, R_m = 12·2±1·76 kΩ cm², C_m = 14·6±3·07 μF/cm².

Non-linear permittivities in 1 mM-tetracaine

Tetracaine has been reported to abolish that steady-state component of non-linear charge, q_γ, whose voltage dependence parallels that of the tension development, in *hypertonic* solutions (Huang, 1981*a*, 1982; Hui, 1982). In this study, adding 1 mM-tetracaine also decreased the low-frequency permittivity and, by inference, the total

amount of non-linear charge (Fig. 8). The discrepancy in the dielectric properties between depolarizing and hyperpolarizing responses was also abolished, and so the frequencies of maximum dielectric loss in both could be represented on a *single* function of potential (Fig. 7*C*). The positions of these peaks were again voltage-

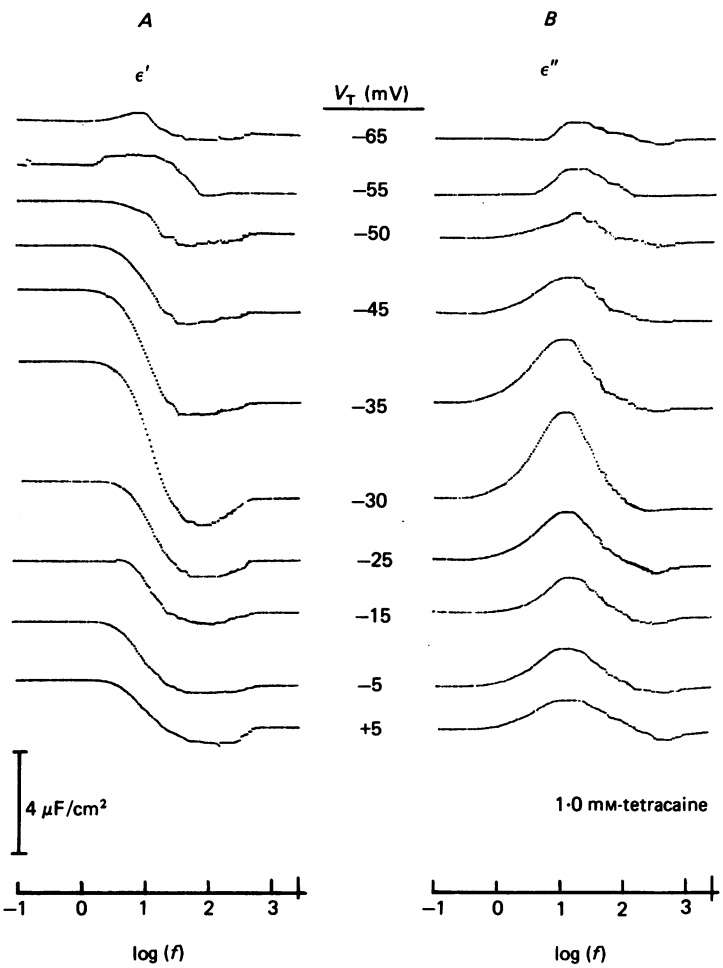

Fig. 8. Dielectric spectra of the non-linear part of *A*, the real, ϵ', and *B*, the imaginary, ϵ'', permittivities at different voltages, V_T, obtained from transients obtained from depolarizing 10 mV steps, in the presence of 1 mM-tetracaine. The frequency scale is the logarithmic one as employed in the previous Figures. Cable constants: R_i, 335 Ω cm; λ, 2·69 mm; r_i, 6246 kΩ/cm; diam. 83 μm; r_m, 451 kΩ cm; R_m, 11·7 kΩ cm², C_m, 17·0 μF/cm².

dependent in that they assumed lower frequencies in the middle of the potential range explored (where the non-linear capacitance measured was largest) than at the ends. However, the positions of the peaks were considerably less dependent on voltage than when tetracaine was absent (Fig. 7*A* and *B*).

The dielectric loss at low frequencies due to q_γ was abolished, as has been reported on an earlier occasion (Huang, 1981*a*) (Fig. 8). This left a single peak only, in both depolarizing or hyperpolarizing responses. In the complex plane, the locus of ϵ''

against ϵ' approximated a simple semicircle (Fig. 9) through the voltages examined. Hence the singularities in the spectra described in previous sections reflect the q_γ rather than the q_β contribution. The results are also consistent with q_β being a simple relaxation of charge between two major energy levels (Duane & Huang, 1982).

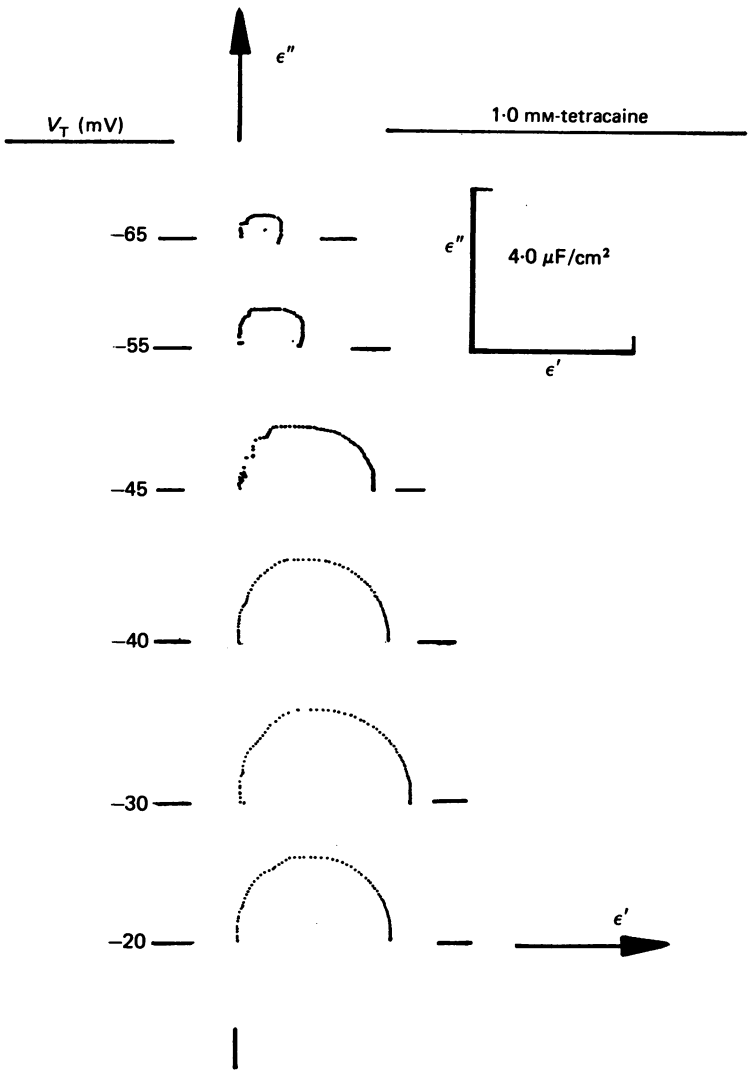

Fig. 9. Complex plane loci describing the complex permittivity as a function of voltage, obtained from depolarizing responses for a fibre in the presence of 1 mM-tetracaine. Cable constants: R_i, 335 Ω cm; λ, 2·21 mm; r_i, 6121 kΩ/cm; diam., 83 μm; r_m, 300 kΩ cm; R_m, 7·87 kΩ cm²; C_m 18·3 μF/cm².

DISCUSSION

This paper presents an analysis of the membrane capacitance in skeletal muscle in terms of the dependence of its complex permittivity upon the frequency. Time domain spectroscopy provided the most straightforward approach in the low

frequencies ($< 10^6$ Hz) concerned (Hill *et al.* 1969). A Fourier transform procedure applied to the transients obtained from small applied potential steps gave the complex permittivities, $\epsilon^* = \epsilon' - j\epsilon''$ and these were presented as functions of frequency in the same way as are the spectra obtained from similar analysis of polymeric materials (Hedvig, 1970). The particular analysis method used here utilized the existence of the required Fourier coefficients that represented the indicial admittances obtained as analytical functions of frequency. This overcame signal theory problems that limited the earlier work (Huang, 1981*a*), in which the Fourier coefficients could only be obtained at discrete and fixed increments of frequency. A detailed representation of the dielectric properties was achieved by choosing a logarithmic frequency abscissa. This gave preferential resolution of the values of the permittivity about the dielectric peaks, yet retained sufficient representation of dispersions at higher frequencies for satisfactory analysis in the complex plane.

It is emphasized that results from approaches of this kind offer a meaningful physical description of the experimental phenomenon only if certain conditions are satisfied. Problems concerning valid representation of the transients have already been discussed in terms of the underlying signal theory. In addition to this the following criteria are necessary.

(1) It is essential that the applied field is uniform over the geometry of the dielectric. For example, attenuations in potential over the membrane through cable effects should be minimal through the range of frequencies examined. This condition has been tested for the three-electrode voltage clamp at frequencies of 0–2·5 kHz in earlier work, (Huang, 1981*b*). This showed that the complex admittance predicted for unit equivalent surface membrane expressed as a function of frequency matched the input admittance deduced for the same circuit in the voltage-clamp geometry considered.

(2) The superposition condition implicit to analysis of the transients requires the indicial admittance to be independent of potential through the voltage step (Weber, 1956). This condition was approximated by using small steps and precludes the use of large applied perturbations in this kind of analysis.

(3) Finally, the system should be time-invariant during the transient response (Papoulis, 1977). Thus, the total available charge should be conserved through the pulse: the Fourier analysis used here should not be applied to systems where charge inactivation is rapid. In skeletal muscle, such charge immobilization has been reported (e.g. Adrian & Almers, 1976*a*), but it occurred over durations well in excess of the pulses described here. Furthermore, conservation of total charge has been satisfied in a wide variety of pulse procedures that occurred in the same time scales as those used here (Adrian & Almers, 1976*b*; Schneider & Chandler, 1973; Huang, 1983).

Given the conditions above, the responses obtained experimentally are actually convolution integrals of the transfer functions of the system with a voltage step. Assuming a capacitative basis for the charge movement, this response is a displacement current and is the derivative of the membrane polarization as a function of time. The transforms obtained therefore represent the transfer functions of the membrane polarization, as well as the complex permittivity in the frequency domain. It may be pointed out that alternative mechanisms involving non-linear conductances in

place of capacitances, have been considered to explain charge movements (Chandler, Rakowski & Schneider, 1976; Matthias, Levis & Eisenberg, 1980). However, specific experimental objections exist for models of this kind, and hence the simplest physical description remains in terms of capacitative charge (Huang, 1983). Also, it appears more likely that the non-linear charge is a direct consequence of a change in applied field rather than one of indirect effects such as binding of released calcium (Horowicz & Schneider, 1981*a*; Huang, 1981*c*). Therefore, q_β and q_γ are most conveniently described in terms of the behaviour of integral membrane polymers exposed to the transmembrane field, as this would be the simplest explanation for such a conserved charge.

The non-linear dielectric dispersion phenomena obtained from frog skeletal muscle occurred at the low frequencies expected for dipole or orientational polarization. As would be expected for polymeric entities subject to sufficiently large fields, the underlying components were characterized by dielectric loss peaks. For example, the q_β component as isolated by adding tetracaine gave a single dielectric loss maximum, whilst its real permittivity declined monotonically with increasing frequency. The semicircular projection of these coefficients in the complex plane suggested that q_β is a relaxing species undergoing transitions between two levels (see also Duane & Huang, 1982) in a simple Eyring system separated by an activated complex. However, although this is the simplest possible interpretation, such a result was in fact not the most expected. One may suppose that charge movements reflect configurational changes involving membrane polymers that are sufficiently large to traverse an appreciable fraction of the membrane thickness. Their over-all dipole moment should then be a vectorial addition of bond moments from a large number of functional groups as referred to the electrical axis. If this is so, a wide variety of transitions, including crankshaft motions of segments of the main chain as well as side group rotations, would be expected. This should produce a large population of relaxation times, resulting in a depressed semicircular arc locus in the complex plane.

In contrast, the straightforward semicircular locus found for q_β implies a single concerted conformational transition. In a polymeric molecule this would result only if there is some degree of steric rigidity constraining the movement of the constituent dipoles relative to each other. This might arise through the secondary or tertiary structure of the polymer, or, alternatively, be the result of the intense transmembrane field. The latter possibility is consistent in a simple way with 'inactivation' of the non-linear charge by prolonged depolarization which then would remove such rigidity (Adrian & Almers, 1976*a*; Adrian, Chandler & Rakowski, 1976). A large number of functional groups involved in a concerted configurational change may explain the considerably lower frequencies at which the experimental dielectric dispersions occur in this system as compared to those found in most aqueous proteins which have frequencies in the MHz range (Takashima & Minikata, 1975).

The possibility of yet additional mechanisms is suggested by the complicated dielectric behaviour of the q_γ component. The steady-state features of q_γ have been described previously in terms of a two-level system with a high minimum valence of about 4·5 (Duane & Huang, 1982). However any simple description in terms of a discrete charge of so high a valency is unlikely to be realistic as it would be unlikely that such an entity can be stable, especially in a medium of low permittivity such

as cell membrane. Additionally, it would then be likely that the actual charge on such a particle would be even higher: the estimate of the effective valency assumed dipole distances normalized to the membrane thickness, and the actual dipole rotations that occur may not involve this entire distance. Furthermore, intense shielding would be expected from the immediate surround of such an intense charge. Finally, a system of more than two levels requires a greater rather than a smaller valency to produce a given degree of potential dependence.

The most realistic available hypothesis in terms of known properties of regulatory molecules would therefore assume that this large charge due to q_γ is distributed between sterically separate sites on the entities concerned, and these somehow interact co-operatively to result in a large over-all potential sensitivity. As the subsystems involved may well be regulatory proteins, the simplest parallels would be with known properties of allosteric enzymes which, through the sensitivity of their conformations to substrate, assume important regulatory functions (Goldbeter & Koshland, 1982; Newsholme & Start, 1972). For example, the underlying canonical subsystems might possess a quaternary structure of several subunits, two or more of which are dependent on electric field.

In a model of the type of Monod, Wyman & Changeux (1965), the over-all, quaternary structure would exist in two possible forms differing in the extent to which alterations in subunit conformation (in this particular system due to changes in the field), are restricted by the steric constraints imposed by their association with their neighbours. This existence of two such principal forms is consistent with the two-level steady-state system proposed by Duane & Huang (1982). Suppose the constrained or associated configuration predominates at the resting potential. A structural transition will occur in one (or more) subunits only with imposition of a sufficiently large depolarization, but, once achieved, will then favour allosteric transition of the entire quaternary structure to the unconstrained (dissociated) form. The remaining subunits in the assembly would then be free to change their conformations and so produce an additional delayed movement of charge reflecting the additional conformational energy made available by the allosteric transition, in addition to that provided by the driving field. This extra charge moved would explain the sharp increase in capacitance (zero-frequency real permittivity), as well as the singularities in the complex plane loci that suggest a movement of charge larger than expected from the corresponding energy dissipation at potentials when q_γ first appears.

These effects would be greatest when most of the subsystems involved are in the constrained form at the foot of the dependence of the non-linear charge upon the voltage: this was indeed observed experimentally. Conversely, these delayed co-operative effects would be less noticeable with stronger depolarization, when the fundamental frequency of the system becomes determined by the more rapid transitions resulting from a field large enough to influence individual subunits directly. This is consistent with the increased frequencies of the dielectric peaks with stronger depolarizations.

In any event, the result of a depolarizing step would be formation of that quaternary structure in which all the constituent subunits are unconstrained, and in which the subunits have altered configurations. Therefore hyperpolarizing return

steps would result in simple monotonic relaxations (as observed experimentally) of now dissociated physical entities, regaining their resting configurations. Thus a description that closely parallels that employed for the action of regulatory proteins such as haemoglobin (Perutz, 1970) can offer a basis upon which experimental findings concerning the charge movement can be explained. However, it is pointed out that this is merely the simplest available model: a number of alternative schemes could well be equally appropriate (e.g. Koshland, Nemethy & Filmer, 1966; Whitehead, 1970).

There is increasing evidence that the q_γ component may be involved in regulating calcium release during contractile activation. There is the sharp appearance of the q_γ dielectric loss peak at potentials close to the contractile rheobase (Huang, 1981*c*; Horowicz & Schneider, 1981*b*), as well as the correspondence of the steady-state charge–voltage relation of q_γ with that of the development of tension (Huang, 1982). Both tetracaine and dantrolene sodium (Huang, 1981*a*, 1982; Hui, 1982) abolish both tension development and q_γ selectively: similar correlations for the other component, q_β, could not be demonstrated. Indeed, optical methods did not detect any increment in intracellular calcium concentrations in response to depolarizations as far as -55 mV: at these voltages, there is an appreciable amount of q_β, but q_γ is absent (Kovacs *et al.* 1979; Huang, 1982). In any event, whatever the detailed physiological role of q_γ, its features certainly imply the presence of mechanisms that would increase its potential sensitivity greatly and so enhance the regulation by voltage of any process it might initiate.

The author would like to thank Dr R. H. Adrian and Dr F. Wray for helpful discussions, and Mr W. Smith for skilled assistance.

REFERENCES

ADRIAN, R. H. (1978). Charge movement in the membrane of striated muscle. *A. Rev. Biophys. Bioeng.* **7**, 85–112.

ADRIAN, R. H. & ALMERS, W. (1974). Membrane capacity measurements on frog skeletal muscle in media of low ionic content. *J. Physiol.* **237**, 573–605.

ADRIAN, R. H. & ALMERS, W. (1976*a*). The voltage dependence of membrane capacity. *J. Physiol.* **254**, 317–338.

ADRIAN, R. H. & ALMERS, W. (1976*b*). Charge movement in the membrane of striated muscle. *J. Physiol.* **254**, 339–360.

ADRIAN, R. H., CHANDLER, W. K. & RAKOWSKI, R. F. (1976). Charge movement and mechanical repriming in skeletal muscle. *J. Physiol.* **254**, 361–388.

ADRIAN, R. H. & PERES, A. (1979). Charge movement and membrane capacity in frog muscle. *J. Physiol.* **289**, 83–97.

BRACEWELL, R. N. (1978). *The Fourier Transform and its Applications*, second edn. New York: McGraw Hill.

CHANDLER, W. K., RAKOWSKI, R. F. & SCHNEIDER, M. F. (1976). A non-linear voltage dependent charge movement in frog skeletal muscle. *J. Physiol.* **254**, 245–283.

COLE, K. S. (1968). *Membranes, Ions and Impulses.* Berkeley: University of California Press.

DEBYE, P. (1929). *Polar Molecules.* New York: Chemical Catalog Co.

DISSADO, L. A. & HILL, R. M. (1979). Non-exponential decay in dielectrics and dynamics of correlated systems. *Nature, Lond.* **279**, 685–689.

DUANE, S. & HUANG, C. L.-H. (1982). A quantitative description of the voltage dependent capacitance in frog skeletal muscle in terms of equilibrium statistical mechanics. *Proc. R. Soc.* B **215**, 75–94.

FALK, G. & FATT, P. (1964). Linear electrical properties of striated muscle fibres observed with intracellular electrodes. *Proc. R. Soc.* B **160**, 69–123.

GOLDBETER, A. & KOSHLAND, D. E. (1982). Sensitivity amplification in biochemical systems. *Q. Rev. Biophys.* **15**, 555–591.

HEDVIG, P. (1970). *Dielectric Spectroscopy of Polymers.* Bristol: Adam Hilger.

HILL, NORA, VAUGHAN, V. E., PRICE, A. H. & DAVIES, M. (1969). *Dielectric Properties and Molecular Behaviour.* New York: Van Nostrand.

HODGKIN, A. L. & NAKAJIMA, S. (1972). The effects of diameter on the electrical constants of frog skeletal muscle fibres. *J. Physiol.* **221**, 105–120.

HOROWICZ, P. & SCHNEIDER, M. F. (1981*a*). Membrane charge movement in contracting and non-contracting skeletal muscle fibres. *J. Physiol.* **314**, 565–593.

HOROWICZ, P. & SCHNEIDER, M. F. (1981*b*). Membrane charge movement at contraction thresholds in skeletal muscle fibres. *J. Physiol.* **314**, 595–633.

HUANG, C. L.-H. (1981*a*). Dielectric components of charge movements in skeletal muscle. *J. Physiol.* **313**, 187–205.

HUANG, C. L.-H. (1981*b*). Membrane capacitance in hyperpolarized muscle fibres. *J. Physiol.* **313**, 207–222.

HUANG, C. L.-H. (1981*c*). Effects of local anaesthetics on the relationship between charge movements and contractile thresholds in frog skeletal muscle. *J. Physiol.* **320**, 381–391.

HUANG, C. L.-H. (1982). Pharmacological separation of charge movement components in frog skeletal muscle. *J. Physiol.* **324**, 375–387.

HUANG, C. L.-H. (1983). Experimental analysis of alternative models of charge movements in frog skeletal muscle. *J. Physiol.* **336**, 527–544.

HUI, C. S. (1982). Pharmacological dissection of charge movements in frog skeletal muscle fibres. *Biophys. J.* **39**, 119–122.

JONSCHER, A. K. (1975). New interpretation of dielectric loss peaks. *Nature, Lond.* **256**, 566–568.

KOSHLAND, D. E., NEMETHY, G. & FILMER, D. (1966). Comparison of experimental binding data and theoretical models in proteins containing subunits. *Biochemistry* **5**, 365–385.

KOVACS, L., RIOS, E. & SCHNEIDER, M. F. (1979). Calcium transients and intramembrane charge movement in skeletal muscle fibres. *Nature, Lond.* **279**, 391–396.

LIGHTHILL, M. J. (1958). *Introduction to Fourier Analysis and Generalized Functions.* Cambridge: University Press.

MATTHIAS, R. T., LEVIS, R. A. & EISENBERG, R. S. (1980). Electrical models of excitation–contraction coupling and charge movement in skeletal muscle. *J. gen. Physiol.* **76**, 1–32.

MONOD, J., WYMAN, J. & CHANGEUX, J. P. (1965). On the nature of allosteric transitions: a plausible model. *J. molec. Biol.* **12**, 88–118.

NEWSHOLME, E. A. & START, C. (1972). General aspects of the regulation of enzyme activity and the effects of hormones. In *Handbook of Physiology* sect. 7: *Endocrinology* **1**, 369–385. Ed. STEINER, D. F. & FREINKEL, N. Washington D.C.: American Physiological Society.

PAPOULIS, A. (1977). *Signal Analysis.* New York: McGraw Hill.

PERUTZ, M. F. (1970). Stereochemistry of co-operative effects in haemoglobin. *Nature, Lond.* **228**, 726–739.

SCHNEIDER, M. F. & CHANDLER, W. K. (1973). Voltage-dependent charge movement in skeletal muscle: a possible step in excitation–contraction coupling *Nature, Lond.* **242**, 244–246.

TAKASHIMA, S. & MINIKATA, A. (1975). Dielectric properties of biological macromolecules. *Dig. Lit. Dielect.* **37**, 602–652.

VON HIPPEL, A. (1954). *Dielectrics and Waves.* New York: John Wiley.

WEBER, E. (1956). *Linear Transient Analysis*, vol. II. New York: John Wiley.

WHITEHEAD, E. P. (1970). The regulation of enzyme activity and allosteric transition. *Prog. Biophys. & molec. Biol.* **21**, 321–398.